# Laser-Induced Magnetization Dynamics of Lanthanide-Doped Permalloy Thin Films

I. Radu,[1,2] G. Woltersdorf,[1] M. Kiessling,[1] A. Melnikov,[3] U. Bovensiepen,[3] J.-U. Thiele,[4] and C. H. Back[1]

[1]*Physics Department, Universität Regensburg, Universitätsstrasse 31, 93040 Regensburg, Germany*
[2]*BESSY GmbH, Albert-Einstein-Strasse 15, 12489 Berlin, Germany*
[3]*Physics Department, Freie Universität Berlin, Arnimallee 14, 14195 Berlin, Germany*
[4]*San Jose Research Center, Hitachi Global Storage Technologies, 3403 Yerba Buena Road, San Jose, California 95135, USA*
(Received 4 July 2008; revised manuscript received 12 February 2009; published 19 March 2009)

We investigate the effect of Ho, Dy, Tb, and Gd impurities on the femtosecond laser-induced magnetization dynamics of thin Permalloy films using the time-resolved magneto-optical Kerr effect. Varying the amount of Ho, Dy, Tb content from 0% to 8%, we observe a gradual change of the characteristic demagnetization time constant from $\approx 60$ to $\approx 150$ fs. In contrast, Gd concentrations up to 15% do not influence the time scale of the initial photoinduced magnetization loss. We propose a demagnetization mechanism that relies on strong magnetic inertia of the rare-earth dopant which stabilizes the ferrimagnetic ordering and thereby delays the demagnetization.

Using femtosecond laser pulses in a pump-probe approach, one can directly address the processes which are responsible for the excitation and relaxation of a magnetic system on their characteristic time scales. Various detection methods have been employed ranging from time-resolved linear magneto-optics [1–3] and nonlinear magneto-optics [4–6] to time-resolved photoemission [6–9]. Very recently time-resolved x-ray magnetic circular dichroism with femtosecond time resolution [10] has been presented. Despite the significant amount of work done on various ferromagnetic materials (e.g., Ni, Fe, Co, CoPt), none of these studies has identified in an unambiguous way the microscopic mechanism responsible for laser-induced demagnetization. On the theoretical side, there have been just a few attempts that address the demagnetization mechanism at a microscopic level [11], still awaiting experimental proof. Recently, Koopmans *et al.* [12] have proposed a demagnetization model inspired by the Elliot-Yafet (EY) spin relaxation mechanism [13] determined by electronic spin-flip scattering mediated by impurities or defects and phonons. Employing quantum mechanical calculations, an analytical expression was derived that connects the demagnetization time constant $\tau_M$ with the Gilbert damping parameter $\alpha$ via the Curie temperature $T_C$ of the system. The theoretical predictions describe the experimental time-resolved magneto-optic Kerr effect (TR MOKE) data obtained on Ni films [12]. In the EY theory spin relaxation occurs via electron scattering at impurities or defects and phonons that are accompanied by spin-flip events. The spin-flip probability is given by the amount of spin mixing of the electronic wave function which in turn is determined by the spin-orbit coupling strength. In a simpleminded picture one might conclude that in the heavy rare-earth elements the spin-orbit interaction is large and thus doping a Permalloy ($Ni_{80}Fe_{20}$) film with rare-earth impurities may be an adequate experimen-

tal approach to study the tunability of the demagnetization time.

In this Letter we test the possibility of altering the demagnetization time of the $3d$ transition metal system Permalloy, by adding magnetic lanthanide (RE) impurities. We investigate the effect of magnetic impurities on the magnetization dynamics of the $Ni_{80}Fe_{20}$ alloy within a combined approach that involves ferromagnetic resonance (FMR) and time-resolved MOKE. Increasing the amount of Ho, Dy, Tb impurities the damping parameter $\alpha$ varies over 2 orders of magnitude. In line with the "slow relaxing impurity" model for RE intermetallics [14,15] and in contrast to an EY-type model, the characteristic time constant of the laser-induced demagnetization process shows a gradual increase with increasing Ho, Dy, Tb concentration. However, for the Gd-doped samples, $\alpha$ as well as the demagnetization time remain unchanged irrespective of the Gd impurity concentration.

Ho-, Dy-, Tb-, and Gd-doped $Ni_{80}Fe_{20}$ thin films of 10 nm (Ho) and 30 nm (Dy, Tb, Gd) thickness, respectively, were deposited by magnetron cosputtering on glass substrates at room temperature. Polycrystalline $Ni_{80}Fe_{20}$ samples with Ho, Dy, Tb content varying from 1% to 8% and with Gd content varying from 5% to 15% were prepared. A seed layer of 2 nm Ta and a cap layer of 2 nm Ta followed by 2 nm Pd were used in all films. The thickness and the impurity content of the films were verified by x-ray reflectivity and Rutherford backscattering. For all dopants the samples are ferrimagnetically ordered with an in-plane magnetization orientation and negligible magnetocrystalline anisotropy, as deduced from static MOKE measurements. The saturation magnetization decreases linearly with increasing impurity concentration.

For the TR MOKE measurements we used a cavity-dumped Ti:sapphire oscillator that delivers 50 fs pulses with an energy of $\approx 42$ nJ/pulse at a repetition rate of 1.52 MHz at 800 nm. The TR MOKE measurements are

performed in the longitudinal geometry with an in-plane external magnetic field of 270 Oe sufficient to saturate the sample. The Kerr rotation is measured in a balanced Wollaston prism configuration with $p$-polarized pump and probe pulses. The probe beam has an incidence angle of 45° with respect to the surface normal; the pump beam is at normal incidence. In all experiments the incident fluence of the pump beam was $\approx 3$ mJ/cm$^2$. The transient MOKE curves are obtained from the difference between the dynamic signals detected for opposite orientations of the magnetization. This procedure eliminates nonmagnetic contributions to the signal (e.g., from transient changes of the optical constants). We have also performed two color experiments (800 nm pump, 400 nm probe) on selected samples which reveal the same transient magnetic behavior. In addition, the transient optical response [linear reflectivity (LR)] of the sample is measured under identical conditions using separate photodiodes. A mechanical chopper modulates the pump beam at a frequency of 480 Hz; the pump-induced changes of the probe beam polarization and intensity are detected using a lock-in technique.

It is instructive to visualize a schematic band structure of the RE-Ni$_{80}$Fe$_{20}$ intermetallic; see Fig. 1(a). In these systems, the $3d$ band of Ni$_{80}$Fe$_{20}$ is strongly hybridized with the $5d$ band of the RE while the $4f$ states lie several electron volts below the Fermi energy. The $3d$-$5d$ exchange interaction is antiferromagnetic leading to an antiparallel alignment of the $3d$ and $4f$ moments. The $5d$-$4f$ coupling can be strongly anisotropic depending on the shape of the $4f$ wave function (which is isotropic for Gd and strongly anisotropic for Ho, Dy, Tb) [16] . Recently, Woltersdorf *et al.* [15] have addressed the RE induced magnetic relaxation mechanism in thin Ni$_{80}$Fe$_{20}$ films which is dominated by the anisotropic $5d$-$4f$ exchange interaction. Detailed FMR measurements at various frequencies and configurations allowed us to deduce the damping parameter $\alpha$ [15] as a function of rare-earth doping. Figure 1(b) summarizes the values of $\alpha$ measured for Ho and Gd impurities. A linear increase of the damping parameter with doping is
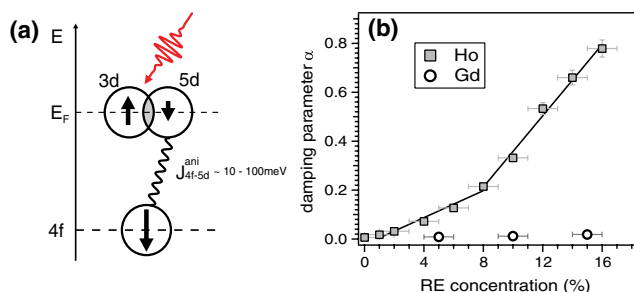
observed according to $\alpha = \alpha_{\text{NiFe}} + \Delta\alpha_{\text{RE}}C_{\text{RE}}$, where $C_{\text{RE}}$ is the RE concentration in percent and $\Delta\alpha_{\text{RE}} = 0.017$ for Ho ($\Delta\alpha_{\text{RE}} = 0.036$ for Dy, $\Delta\alpha_{\text{RE}} = 0.038$ for Tb, not shown, see [15]). For Ho concentrations higher than 8% a change in the slope of $\alpha$ is observed. This effect is related to a structural transition of the sample from polycrystalline to amorphous state [17]. We have thus limited our time-resolved measurements to samples with an impurity content of 8% Ho, Dy, Tb and below. Gd doping affects the damping only very weakly with $\Delta\alpha_{\text{RE}} = 0.0005$.

Since the involved time scales for photoinduced demagnetization processes are typically in the range of few tens of femtoseconds our experiment requires a precise determination of the pump-probe zero delay and of the laser pulse duration. For this purpose we have used the so-called "coherent artifact" effect [18] which arises from the interference between the pump and probe pulses during their spatial and temporal overlap. The coherent artifact appears in the LR signal as a pronounced oscillatory component close to zero delay; see Fig. 2. The pure coherent artifact contribution is obtained by differentiating the transient LR signal as displayed in the inset of Fig. 2. Fitting the envelope with a Gaussian profile we obtain a pulse duration of 50 fs at the sample position.

Figure 3 shows the dynamic magneto-optical response of the Ho- and Gd-doped Ni$_{80}$Fe$_{20}$ samples. Each dynamic MOKE curve is normalized to its peak value and down-shifted by one unit for clarity. Note that the maximum demagnetization increases linearly as a function of doping concentration from about 3% up to about 10% for a Ho impurity concentration of 6% and to about 9.5% for a Gd concentration of 10%. This effect is a consequence of the reduced reflectivity with increasing RE doping and will be discussed elsewhere. The decreased reflectivity leads to an increase of the dc heating with increasing doping. dc heating manifests itself in a vertical shift of the measured transient curves from the zero level as indicated by the dash-dotted line in Fig. 3. The maximum dc heating effect for the sample with 15% Gd doping amounts to about 30 K.
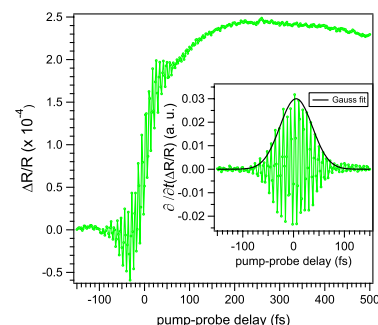
FIG. 1 (color online).  (a) Illustration of the energy levels of the $3d$, $5d$, and $4f$ levels of the RE-doped Ni$_{80}$Fe$_{20}$ films. In the pump-probe experiment we predominantly excite the Ni$_{80}$Fe$_{20}$ $3d$ electrons. (b) The variation of the Gilbert damping parameter $\alpha$ with the concentration of Ho and Gd impurities, as measured by FMR. The black lines are guides to the eye.

FIG. 2 (color online).  Pump-induced changes in the linear reflectivity measured on the pure Ni$_{80}$Fe$_{20}$ sample. The pronounced oscillatory component is the signature of the coherent artifact. Its contribution is separated by differentiating the transient LR signal as displayed in the inset. The solid line is a Gaussian fit to the data which gives a pulse length of 50 fs.
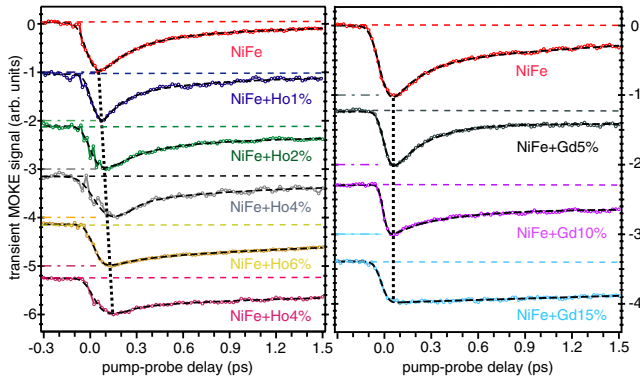
FIG. 3 (color online). Time-resolved MOKE response measured on pure $Ni_{80}Fe_{20}$ and Ho- and Gd-doped $Ni_{80}Fe_{20}$ samples. The dash-dotted horizontal lines indicate the zero level of the transient signal, while the dashed line indicates the unpumped signal measured at negative delays. The black dotted lines illustrate the gradual tendency of the extremum position of the TR MOKE transients to longer pump-probe delays for Ho, while for Gd the position remains unchanged.

All transient MOKE curves have two features in common: (i) a rapid drop of the transient signal within the first hundred femtoseconds after laser excitation, which is ascribed to an ultrafast loss of magnetization, and (ii) a partial recovery of the transient signal to an intermediate level on a picosecond time scale. As the Ho doping is increased, we observe that it takes longer to demagnetize the system. This is deduced from the gradual change in the slope of the initial drop and from the shift of the extremum position to longer pump-probe delays, as indicated by the black dotted line in Fig. 3.

The remagnetization on the picosecond time scale shows a similar behavior: the remagnetization time increases steadily from $\approx 0.35$ ps for $Ni_{80}Fe_{20}$ to $\approx 1$ ps for $Ni_{80}Fe_{20}$ doped with 8% Ho. For the demagnetization of the Gd-doped samples we observe a different behavior compared to the Ho-doped samples: The demagnetization time is constant and does not change even for a relatively high concentration value of 15%. On the other hand, the remagnetization times of the Gd-doped samples follow the same behavior as observed for Ho, i.e., increasing remagnetization times with increasing dopant concentrations.

In order to retrieve the characteristic time constants of these two processes we have used the following phenomenological fit function [2,19]:

$$f(t) = H(t)[A(1 - e^{-t/\tau_M})e^{-t/\tau_R} + B(1 - e^{-t/\tau_R})]. \quad (1)$$

Here $H(t)$ is the Heaviside step function, $\tau_M$ and $\tau_R$ are demagnetization and remagnetization time constants, respectively, while $A$ and $B$ are the exponential amplitudes with $B \ll A$. The above expression is convoluted with a Gaussian that accounts for the finite time resolution of the experiment. As can be seen in Fig. 3, the fit function describes the measured data well.

The demagnetization time $\tau_M$ as a function of RE impurity concentration is plotted in Fig. 4. In the same figure we show for comparison the predicted values of $\tau_M$ deduced for Ho and Gd doping according to the model of Koopmans et al. [12]. $\tau_M$ has been calculated by inserting the measured values of $\alpha$ and the estimated Curie temperatures of Ho- and Gd-doped samples [20] into Eq. (7) of Ref. [12]. The measured $\tau_M$ varies from $\approx 60$ fs for pure $Ni_{80}Fe_{20}$ to a value of $\approx 175$ fs for 4% Ho. Exactly the *opposite* behavior is expected according to Koopmans's prediction: starting with hundreds of femtoseconds for pure $Ni_{80}Fe_{20}$, $\tau_M$ should decrease rapidly for 2% of Ho doping and reach a few femtoseconds at a doping level of 8%. The latter behavior reflects mainly the variation of $\alpha$ as a function of doping concentration. In contrast, Gd doping leads to no change of the demagnetization time within the experimental error. Here we note that the highest Gd-doping values are higher by a factor of 2 compared to the Ho case. Also for this system our findings are at variance with Koopman's predictions (empty circles in Fig. 4). Figure 4 also includes data points for Tb and Dy doping which show the same trend as the Ho data, a gradual increase as a function of doping level.

At this point we would like to note that in a recent Letter no change of the demagnetization time with Dy doping (1% and 2%) has been observed [21] at much higher fluences of 40 mJ/cm². The reported demagnetization times have been determined to be around 200 fs for pure Permalloy and for Dy-doped films. We would also like to mention that in this study the contributed damping due to Dy doping is considerably smaller than what has been observed in [15].

In the following we will discuss the possible origin of the observed photoinduced demagnetization behavior.

First we address the change of the electronic structure by increasing doping. The enhanced effective absorption of
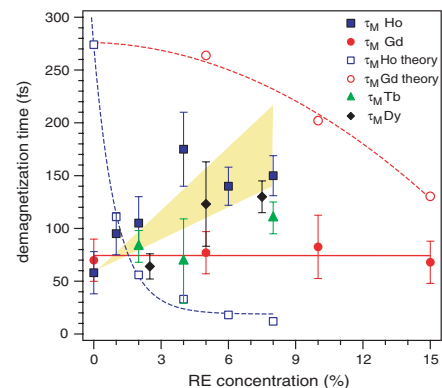


FIG. 4 (color online). Change of the demagnetization time constant $\tau_M$ with Ho, Dy, Tb, and Gd impurity content. The empty symbols represent the calculated values of $\tau_M$ for the case of Ho and Gd doping according to [12]. All curves are guides to the eye. The yellow triangular area corresponds to the region which can be expected from the slow relaxing impurity model for Ho, Dy, and Tb.

the samples upon doping is equivalent to an enhanced excitation that results in an increased pump-induced demagnetization value, i.e., similar to increasing the laser fluence. It has been observed previously that increasing the laser fluence slows down the demagnetization process [9,22]. Thus, in our case, the degree of demagnetization should follow the magnitude change of the linear reflectivity. This is not observed in the experiments. Instead, we observe that this magnitude decreases with RE doping and saturates at about 4% of RE doping while the normalized demagnetization amplitude continuously increases from $\approx 3\%$ to 10% by going from pure $Ni_{80}Fe_{20}$ to 8% of Ho doping. Moreover, a very similar behavior of the linear reflectivity is observed for Gd-doped samples where the demagnetization time constant is not affected at all. Hence, we can exclude that the enhanced absorption due to RE doping is responsible for the increased demagnetization time as a function of concentration in the Ho-, Dy-, and Tb-doped samples.

A more probable explanation of the demagnetization behavior is based on the "slow relaxing impurity model" which perfectly describes the magnetic relaxation at GHz frequencies in RE-$Ni_{80}Fe_{20}$ intermetallics [14,15]. In this model the relevant ingredients are (i) the effectively anisotropic exchange coupling of the RE $4f$ magnetic moments to the $3d$ moment of the transition metals and (ii) the thermal population of the $4f$ states which are exchange split due to the $4f$-$5d$ exchange field. The anisotropy of the effective $4f$-$3d$ exchange interaction causes a modulation of the $4f$ exchange splitting when the $3d$ magnetic moment precesses. The thermal population of these $4f$ levels follows this modulation, but is delayed by the RE spin lattice relaxation time. This mechanism leads to the very large magnetic damping in Ho-, Dy-, and Tb-doped $Ni_{80}Fe_{20}$. Following this model, rapid changes of the $3d$ magnetic moment are projected onto the $4f$ moment, albeit with a time delay given by the rare-earth relaxation time. This relaxation time is of the same order for the studied impurities Ho, Dy, and Tb and amounts to about 1 ps at room temperature [15,23]. We consider the quenching of the transition metal magnetization as a local randomization of the $3d$ magnetic moments (which is a crude approximation but may capture the essential physics). On a microscopic level this would imply that the effective $3d$-$4f$ exchange field acting on the $4f$ moments changes in the case of Ho, Dy, and Tb (which have an anisotropic $5d$-$4f$ exchange interaction), but remains constant in the isotropic case of Gd. For this reason, in the anisotropic case the demagnetization time is delayed by 1 ps due the magnetic inertia which is caused by the time required for the repopulation of the $4f$ levels. In contrast, for the isotropic case no effect on the demagnetization time is expected in agreement with our experimental findings. The triangular area in Fig. 4 is computed by mixing a slow relaxation time (between 1 and 2 ps) according to the RE concentration with the fast demagnetization time of pure $Ni_{80}Fe_{20}$.

In summary, we have studied the effect of Ho, Dy, Tb, and Gd impurities on the magnetization dynamics of thin Permalloy films employing ferromagnetic resonance and time-resolved magneto-optics. Ho, Dy, and Tb change the damping parameter drastically and slow down the photo-induced demagnetization process. In contrast, Gd does not affect the damping parameter and the demagnetization time. Our results are in quantitative and qualitative disagreement with the theoretical predictions of a demagnetization mechanism relying on impurity-assisted spin-flip scattering proposed by Koopmans *et al.* which seems to be oversimplified for the case of $4f$ impurities. This leads us to the conclusion that the dominant fast relaxation process is slowed down by adding slow relaxing impurities. Hence, the simple model of Ref. [12] does not describe our observations.

[1] E. Beaurepaire, J.-C. Merle, A. Daunois, and J.-Y. Bigot, Phys. Rev. Lett. **76**, 4250 (1996).
[2] L. Guidoni, E. Beaurepaire, and J. Y. Bigot, Phys. Rev. Lett. **89**, 017401 (2002).
[3] B. Koopmans, M. van Kampen, J. T. Kohlhepp, and W. J. M. de Jonge, Phys. Rev. Lett. **85**, 844 (2000).
[4] J. Hohlfeld, E. Matthias, R. Knorren, and K. H. Bennemann, Phys. Rev. Lett. **78**, 4861 (1997).
[5] H. Regensburger, R. Vollmer, and J. Kirschner, Phys. Rev. B **61**, 14 716 (2000).
[6] M. Lisowski *et al.*, Phys. Rev. Lett. **95**, 137402 (2005).
[7] A. Scholl, L. Baumgarten, R. Jacquemin, and W. Eberhardt, Phys. Rev. Lett. **79**, 5146 (1997).
[8] H.-S. Rhie, H. A. Dürr, and W. Eberhardt, Phys. Rev. Lett. **90**, 247201 (2003).
[9] M. Cinchetti *et al.*, Phys. Rev. Lett. **97**, 177201 (2006).
[10] C. Stamm *et al.*, Nature Mater. **6**, 740 (2007).
[11] G. P. Zhang and W. Hübner, Phys. Rev. Lett. **85**, 3025 (2000).
[12] B. Koopmans, J. J. M. Ruigrok, F. Dalla Longa, and W. J. M. de Jonge, Phys. Rev. Lett. **95**, 267207 (2005).
[13] Y. Yafet, in *Solid State Physics*, edited by F. Seit and D. Turnbull, Vol. 14 (Academic, New York, 1963), pp. 1–98.
[14] J. H. van Vleck and R. Orbach, Phys. Rev. Lett. **11**, 65 (1963).
[15] G. Woltersdorf *et al.*, http://xxx.lanl.gov/abs/0802.3206v3.
[16] Yu. P. Irkhin, Sov. Phys. JETP **154**, 321 (1988).
[17] W. Bailey, P. Kabos, F. Mancoff, and S. Russek, IEEE Trans. Magn. **37**, 1749 (2001).
[18] M. V. Lebedev, O. Misochko, T. Dekorsy, and N. Gerogiev, JETP **100**, 272 (2005).
[19] N. Del Fatti *et al.*, Phys. Rev. B **61**, 16 956 (2000).
[20] $T_C$ of the alloy is deduced from the weighted average of the $Ni_{80}Fe_{20}$ and RE dopant Curie temperatures.
[21] J. Walowski *et al.*, Phys. Rev. Lett. **101**, 237401 (2008).
[22] M. van Kampen, Ph.D. thesis, Eindhoven University, 2003.
[23] B. H. Clarke, Phys. Rev. **139**, A1944 (1965).